



ISSN: 0067-2904

## Reduction of Radioactive Cesium Concentration in Water Using Iron Oxide Nanoparticles

Ahmed H. Ali, Asia H. Al-Mashhadani\*

Department of Physics, College of Science, University of Baghdad

Received:12/6/2024

Accepted:22/12/2024

Published: 30/1/2026

### Abstract

The work focuses on the pressing issue of pollution caused by radionuclides, which causes significant hazards to humans, public health and the environment. Radioactive cesium (Cs) is among these pollutants. It is particularly hazardous due to its high mobility and long half-life (30 years). To remove cesium from radioactive waste, traditional treatment methods were used, such as ion exchange and coagulation, both generate large quantities of radioactive sludge and are energy-intensive. To overcome this problem, a method can be employed using nano-adsorbents, such as iron oxide-based materials like magnetite. This research explores the application of iron oxide nanoparticles ( $Fe_3O_4$ ) as a novel approach to remove radioactive cesium (Cs) from contaminated water. The use of nano-adsorbents represents a more efficient and sustainable option.

This work examines the removal of Cs from water using nanoparticles ( $Fe_3O_4$ ) and magnetic separation. Iron oxide nanoparticles were synthesized via a chemical co-precipitation method and characterized using various techniques, including Field Emission Scanning Electron Microscopy (FESEM), X-ray diffraction (XRD), Fourier Transform Infrared Spectroscopy (FTIR), Energy Dispersive X-ray Spectroscopy (EDX), and Atomic Force Microscopy (AFM). The results approved the successful preparation of nano- $Fe_3O_4$  with desired properties, such as morphology, functionalization, and crystalline structure.

Adsorption parameters, such as contact time, pH, initial activity, and concentration, were experimentally investigated. The adsorption efficiency of Cs removal increased with increasing the mass of nano- $Fe_3O_4$ , with an optimal removal value of 0.5g of adsorbent. Furthermore, the study examined aqueous pH and the influence of Cs-137 specific activity on the remediation treatment, showing promising results under different conditions. The Cs removal efficiency of 84.79% was notably maximum at 0.5g adsorbent mass with a pH of 9. Additionally, the effect of contact time on the remediation treatment was investigated revealing maximum removal efficiency at 1440 minutes, after which it plateaued. These results underscore the efficacy of  $Fe_3O_4$  nanoparticles in capturing Cs from aqueous solutions, which makes it easier to remove radioactive waste.

Using iron oxide nanoparticles as effective sorbents for processing radioactive materials,  $^{137}Cs$ -contaminated water, proved to be a promising way to mitigate environmental impacts and health hazards associated with radionuclide contamination.

**Keywords:** Removal of Cs, water, iron oxide nanoparticles , adsorption

\*Email: [asia.hammad@sc.uobaghdad.edu.iq](mailto:asia.hammad@sc.uobaghdad.edu.iq)

## تقليل تركيز السبيزيوم المشع في الماء باستخدام جزيئات أكسيد الحديد النانوية

احمد حسين علي، اسيا حميد حمد\*

قسم الفيزياء ، كلية العلوم، جامعة بغداد

### الخلاصة

تركز الدراسة الحالية على معالجة مشكلة التلوث الناتج عن النظائر المشعة التي تشكل تهديد كبيه للصحة العامة والبيئة على الصعيد العالمي. ومن بين هذه الملوثات، فإن السبيزيوم الإشعاعي ( $\text{Cs}$ ) يعتبر خطيرًا بشكل خاص بسبب حركته العالية وطول عمر النصف له. وتعتبر الطرق التقليدية لإزالة السبيزيوم من النفايات الإشعاعية، مثل التكتل وتبادل الأيونات، كلاهما يستهلكان الطاقة بكثافة ويولدان كميات كبيرة من التلوث الإشعاعي. ولمواجهة هذه المشكلة، هناك اهتمام متزايد في استخدام الجسيمات النانوية الممدصة ، وبالتحديد المركبات البارامغنتية مثل أكسيد الحديد. تتناول هذه الدراسة استخدام جزيئات أكسيد الحديد النانوية ( $\text{Fe}_3\text{O}_4$ ) كوسيلة مبتكرة لإزالة السبيزيوم المشع ( $\text{Cs}$ ) من المياه الملوثة. بخلاف الطرق التقليدية التي تتطلب طاقة كبيرة وتنتج كميات هائلة من النفايات، فإن اعتماد المواد النانوية الماسحة يمثل خيارًا أكثر كفاءة واستدامة .

استخدمت جسيمات أكسيد الحديد وطريقة الفصل المغناطيسي في البحث الحالي لإزالة السبيزيوم من المياه. وتم تحضير جسيمات أكسيد الحديد النانوية بطريقة الترسيب الكيميائي المشترك وتم توصيفها باستخدام تقنيات مختلفة بما في ذلك تقاضل الانعكاس السيني ( $\text{XRD}$ )، والمجهر الإلكتروني الماسح ( $\text{FeSEM}$ )، والشنت الإشعاعي للأشعة السينية ( $\text{EDX}$ )، وتحويل فوري للتحويلات ( $\text{FTIR}$ )، ومجهر القوة الذري ( $\text{AFM}$ ) . وأكدت النتائج نجاح تحضير نانو- $\text{Fe}_3\text{O}_4$  بالخصائص المطلوبة مثل حجم البلورات والهيكل البلوري والشكل الخارجي . استقصت التحقيقات التجريبية للمعلمات الخاصة بالامتصاص بما في ذلك الحموضة و زمن الاتصال والتركيز الابتدائي وجرعة الكتلة. زادت كفاءة امتصاص السبيزيوم مع زيادة كتلة نانو- $\text{O}_4\text{Fe}_3$ ، مع تحقيق إزالة مثلى عند استخدام 0.5 جرام من المتصاص. بالإضافة إلى ذلك، فإن الدراسة فحصت تأثير نشاط السبيزيوم-137 النوعي والحموضة المائية على عملية التتقية، مما أظهر نتائج مشجعة تحت ظروف متغيرة. كانت كفاءة إزالة السبيزيوم مرتفعة بشكل ملحوظ عند  $\text{pH}$  يساوي 9 وبلغت 84.79٪ باستخدام كتلة ممتصصة قدرها 0.5 جرام.

علاوة على ذلك، تم استكشاف تأثير زمن الاتصال على عملية التتقية، حيث كشف البحث أن الكفاءة القصوى للإزالة تم تحقيقها في 1440 دقيقة، بعد ذلك بدأت تتلاشى. تؤكد هذه النتائج فعالية جسيمات  $\text{Fe}_3\text{O}_4$  في الاستياء الانتقائي على السبيزيوم من الحلول المائية، مما يسهل إزالتها من النفايات الإشعاعية. بشكل عام، تسلط الدراسة الضوء على إمكانيات جسيمات أكسيد الحديد كمتصاصات فعالة لتنقية المياه الملوثة بالسببيزيوم الإشعاعي، مما يقدم طريقة واعدة للتخفيف من المخاطر البيئية والصحية المرتبطة بالتلويث بالنظائر المشعة.

### Introduction

Pollution from radionuclides, heavy metals, and pesticides has been a growing problem for public health around the world in recent decades [1]. Radionuclides are substances that release neutrons,  $\alpha$ -rays,  $\beta$ -rays, or both. Radioactive cesium ( $\text{Cs}$ ), due to its high specific radioactivity and lengthy half-life, is among the most dangerous and problematic radionuclides [1,2]. Leakage of  $\text{Cs}$  can have serious consequences for both humans and the environment because of its extremely high mobility as a result of its remarkable dissolving properties in water [3]. A lot of attention in nuclear industry and research has been concentrated on removing cesium isotopes ( $^{134}\text{Cs}$ ,  $^{135}\text{Cs}$ , and  $^{137}\text{Cs}$ ) from radioactive waste.

A major portion of the radioactivity found in spent nuclear fuel waste is attributed to cesium radioisotopes, which have a long half-life and generate powerful gamma radiation. Conventional treatment methods, such as coagulation, precipitation, and ion exchange, consume high energy and generate significant quantities of radioactive sludge. The utilization of nano-adsorbents in the purification of radioactive water is rapidly garnering attention. An adsorbent used for water remediation must possess a substantial adsorption capacity, as well as excellent physical and chemical stability, a significant surface area, non-toxicity, high recyclability, and easy separability. The carbon-based superparamagnetic composite adsorbents significantly decrease solid waste generation due to their remarkable removal capabilities, which are influenced by several parameters, such as their remarkably large surface area, magnetic susceptibility, and great chemical stability. The use of iron oxide-based adsorbents, such as magnetite ( $Fe_3O_4$ ), hematite ( $\alpha-Fe_2O_3$ ), and magnetic magnetite ( $\gamma-Fe_2O_3$ ), has gained significant interest due to their low cost, simple preparation, non-toxicity, ability to attract water, ease of separation, and excellent performance in adsorbing As ions[4,5].

Several researches have highlighted the potential of iron oxide nanoparticles as a promising solution for mitigating environmental impacts associated with radionuclide contamination, offering a more sustainable and efficient approach to radioactive waste management [6-8]. Previous studies have examined several nanomaterials, including nano natural material [9], magnetic nanocomposite material [10], and nano herbs (specifically turmeric) [11], to diminish the impact of radioactivity. Additionally, there exist alternative methods for treating the long-lasting radionuclides, such as employing thermal neutron interaction or gamma rays [12,13], or developing specific materials or shielding [14].

In this work, magnetite (iron oxide,  $Fe_3O_4$ ) was used to remove Cs from contaminated water, collected from the Tuwaitha nuclear site. Iron oxide was prepared by chemical co-precipitation method. Cs is adsorbed on iron oxide nanoparticles and this was separated using a magnet, thus reducing the amount of Cs. The effect of the adsorption parameters, including pH, contact time, initial concentration, and mass of absorbed material (nano  $Fe_3O_4$ ) were studied.

## Material and Method

The materials used in this work were ferric chloride anhydrous ( $FeCl_3$ ), ferrous sulphate heptahydrate ( $FeSO_4$ ), and  $NH_3(25\%)$ . XRD, FESEM + EDX, FTIR, BET and gamma spectroscopy with high purity germanium detector were used for characterization. Magnetite ( $Fe_3O_4$ ) was prepared by adding  $FeCl_3$  to  $FeSO_4$  with ammonia solution according to the following chemical reaction:



## Experimental Work

Using chemical co-precipitation method, the  $Fe_3O_4$  nanoparticles were synthesized according to the chemical reaction with a weight ratio of  $FeSO_4$  (II): iron (III) chloride of two:one. 5.4 g of  $FeSO_4$  (II), 2.78 g of iron (III) chloride, and 250 mL of distilled water were dispersed in a beaker using ultra sonication. At 70 °C, homogenization was performed by adding 20 mL of ammonia solution dropwise until the pH of the solution reached 9. At a pH of about 9, a black precipitate containing magnetic nanoparticles was formed. The formed precipitate was stirred for 2700s. It was then swilled several times with double distilled water to remove impurities. Finally, magnetite ( $Fe_3O_4$ ) nanoparticles were separated using a 1.3

Tesla magnet, dried for 720min and then heated in containers in an oven at 70 °C. Figure 1 shows the decontamination process of the Cs-contaminated water.



**Figure 1:** The decontamination process of the Cs-contaminated water

## Results and Discussion

Nano- $\text{Fe}_3\text{O}_4$  was characterized using different methods such as XRD, FESEM, EDX, FTIR, UV-Vis, AFM and BET.

### 1- XRD analysis

The crystalline properties were characterized by X-ray diffraction (XRD) using a Siemens D5000 diffractometer. The diffractogram was obtained using  $\text{Cu-K}\alpha$  radiation ( $\lambda=1.5406 \text{ \AA}$ ) in the range  $10^\circ < 2\theta < 80^\circ$  with steps of  $0.02^\circ$  and acquisition time of  $1.0 \text{ s/step}$ . Fig. 2 shows the XRD pattern of the prepared nano  $\text{Fe}_3\text{O}_4$  by the chemical co-precipitation method. From this figure, many characteristic peaks were observed at  $(2\ 2\ 0)$ ,  $(3\ 1\ 1)$ ,  $(4\ 0\ 0)$ ,  $(4\ 2\ 2)$ ,  $(5\ 1\ 1)$ , and  $(4\ 4\ 0)$ , which are in accordance with the inverse cubic spinel phase of  $\text{Fe}_3\text{O}_4$  (magnetite, according to JCPDS card no. 85-1436). These results are similar to those reported in the literature [15]. The sharp XRD peaks indicates that the mean crystallite diameter of the nano  $\text{Fe}_3\text{O}_4$  was around (10 nm).

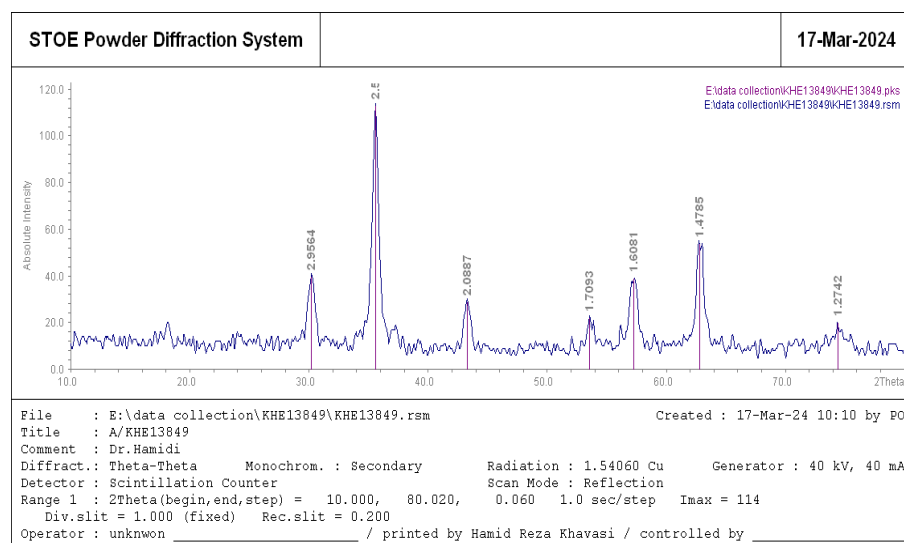


**Figure 2:** XRD pattern of nano  $\text{Fe}_3\text{O}_4$  prepared by chemical co-precipitation method.

## 2. FESEM analysis

Fig. 3 shows the surface morphology of the nano  $\text{Fe}_3\text{O}_4$  as observed by the FESEM micrographs; as seen, most of the nanoparticles were quasi-spherical. From the micrographs using Scherrer's formula, the mean crystal size was around 10 nm. The sharp peaks of the XRD patterns confirm this result.

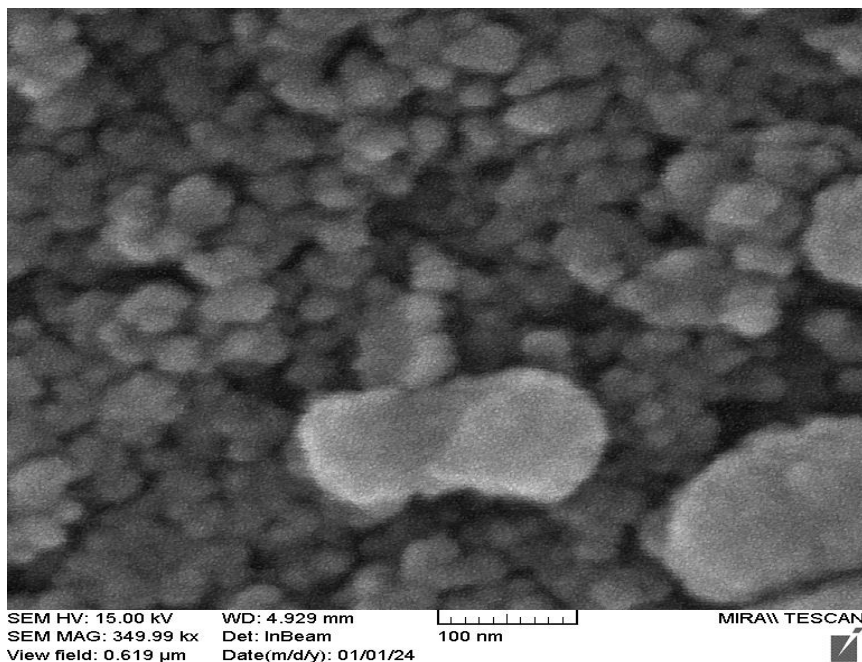


**Figure 3:** FESEM micrographs of nano  $\text{Fe}_3\text{O}_4$

### 3. FTIR analysis

The function of the magnetite nanoparticles was studied using FT-IR spectroscopy. Fig. 4 shows the FT-IR spectrum of magnetite. The prominent peak around  $571 \text{ cm}^{-1}$  is attributed to the Fe–O bond vibration, which is characteristic of the magnetite core structure ( $\text{Fe}_3\text{O}_4$ ). This confirms the presence of the magnetic core, which is the fundamental feature of magnetite nanoparticles. The position of this peak indicates the presence of  $\text{Fe}_3\text{O}_4$  in the sample, emphasizing the magnetic properties of the material.

The wide absorption band around  $3400 \text{ cm}^{-1}$  compatible to the stretching vibration of groups (OH) present in water or on the surface of the nanoparticles. This suggests that the nanoparticles are either hydrophilic, indicating the presence of surface-bound hydroxyl groups, which are common in magnetite nanoparticles due to their interaction with functional groups in the surrounding medium.

The spectrum of FT-IR confirms the conclusion that the magnetite nanoparticles have been functionalized with oleic acid. All peaks associated with the C–H stretches and the Fe–O bond indicate that oleic acid molecules are likely adsorbed on the surface of the  $\text{Fe}_3\text{O}_4$  nanoparticles.

This functionalization can improve the dispersion of nanoparticles in organic solvents and enhance their stability in different environments.

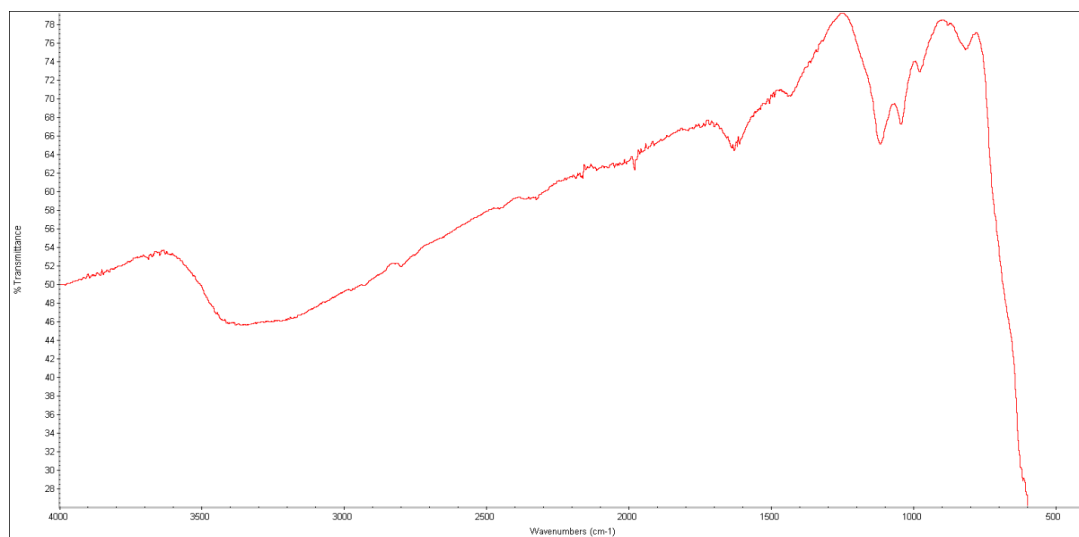


**Figure 4:** The FT-IR spectrum of nano  $\text{Fe}_3\text{O}_4$  magnetite

#### 4. AFM analysis

The surface roughness and topography of the deposited thin films were evaluated from the micrographs of an atomic force microscope (Digital Instruments Inc. Nanoscope 3 and Dimension 3100). The roughness and grain size from the AFM images were measured using the root mean square (RMS) method. Atomic force microscopy was utilized to determine the morphology and size of the prepared nano  $\text{Fe}_3\text{O}_4$ . The prepared  $\text{Fe}_3\text{O}_4$  nanoparticles have an average diameter of 47.43nm. Figure 5 shows AFM images along with particle size distribution histograms. The particles are nanosized and somewhat spherical.

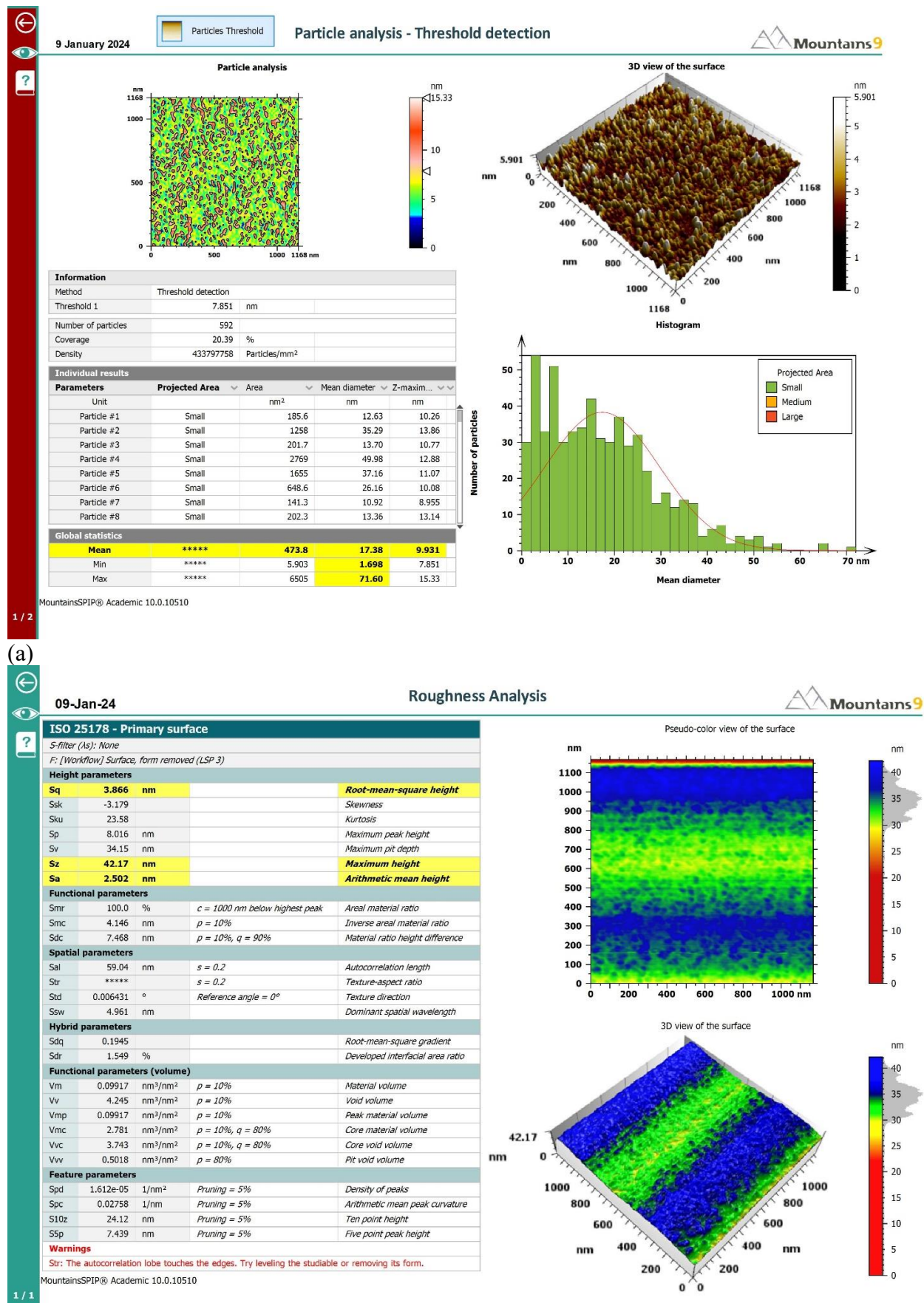


Figure 5:(a,b) : AFM images along with particle size distribution histograms for nano Fe<sub>3</sub>O<sub>4</sub>

### 5- Effect of adsorbent mass

The first experiment was to study the effect of the adsorbent mass on the removal efficiency. The mass of the adsorbent was varied between (0.0-0.5) g. This was done with 10ml volume of the contaminated water at a constant pH of 7. The time of contact of nano  $\text{Fe}_3\text{O}_4$  with Cs-137 radionuclides of 1440 min., the count rate of the Cs-contaminated water before adding the adsorbent (nano  $\text{Fe}_3\text{O}_4$ ) ( $C_e$ ) was 2315 Bq/l. Table 1 presents the sample code, the adsorbent(nano  $\text{Fe}_3\text{O}_4$ ) mass (g), the count rate for the peak for the different adsorbent masses ( $C_f$ ) and the reduction percentage for Cs-137 from water.

**Table 1:** The sample code, the mass of adsorbent (nano  $\text{Fe}_3\text{O}_4$ )(g), the count rate before treatment with nano  $\text{Fe}_3\text{O}_4$  ( $C_e$ ) is 2315 Bq/l, the count rate at the peak( $C_f$ ) and the reduction percentage for Cs-137 radionuclides from water.

Code	Wt. of Adsorbent (g)	$C_f$ Bq/l	$R\% = \frac{C_e - C_f}{C_e} \times 100$
AF1	0.1	580	74.95
AF2	0.2	531	77.06
AF3	0.3	431	81.38
AF4	0.4	358	84.53
AF5	0.5	352	84.79

The adsorption kinetic parameters are also necessary to the functional application of the nano adsorbent. The Cs removal efficiency was calculated as a function of nano adsorbent mass (0.0-0.5g) to determine the optimum amount of adsorbent for the decontamination experiments (Figure 6). The adsorption efficiency of Cs increases with the increase in the mass of nano  $\text{Fe}_3\text{O}_4$  used. The highest adsorption efficiency was observed when 0.5g of nano  $\text{Fe}_3\text{O}_4$  was used, resulting in percentage reduction of 84.79%. The adsorption of Cs was rapid in the first 0.4g of nano  $\text{Fe}_3\text{O}_4$ , indicating that most of the adsorption occurs within this range. This rapid adsorption could be due to the high surface area and reactivity of the nano  $\text{Fe}_3\text{O}_4$ . Then, after 0.4g, the adsorption rate slowed down, and the adsorption efficiency plateaued. This suggests that the adsorbent sites are fully occupied, and a further increase in the adsorbent mass does not significantly enhance the adsorption efficiency.

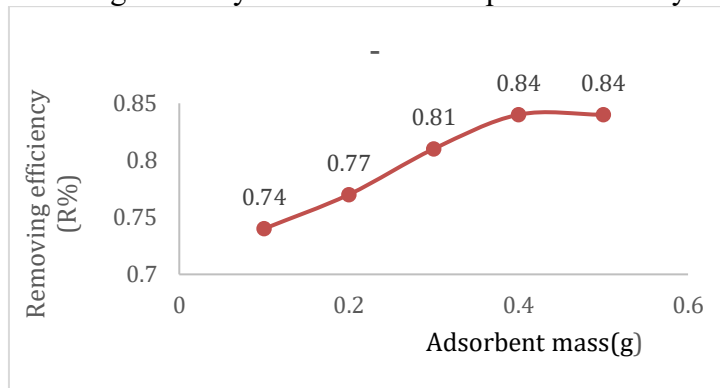


**Figure 6:** Absorption kinetics as a function of adsorbent mass

### 6-Effect of specific activity of Cs-137 on the remediation process of radioactive waste

To investigate the industrial range of remediation process of radioactive waste, addition optimization and validation of the process were done. In this experiment Cs removal efficiency was measured at various Cs specific activity values (500-4000 Bq/ml) at constant

pH value, constant absorbent mass of (0.5g) and constant contact time between nano  $\text{Fe}_3\text{O}_4$  and Cs ions of (1440 min.). Table 2 presents the sample code, the count rate at the peak before treatment with nano  $\text{Fe}_3\text{O}_4$  ( $C_e$ ), the count rate at the peak after treatment with nano  $\text{Fe}_3\text{O}_4$  ( $C_f$ ) and the reduction percentage for Cs-137 radionuclides from water.

**Table 2:** The sample code, the count rate at the peak and the percentage reduction of Cs-137 radionuclides from water at constant pH (7), the adsorbent mass (nano  $\text{Fe}_3\text{O}_4$ )(0.5g), the volume (10ml) of Cs-137, and constant contact time between nano  $\text{Fe}_3\text{O}_4$  and Cs ions (1440 min)

Samples	( $C_e$ ) Bq/ml	$C_f$ Bq/ml	R(%)
CF1	500	315	37.0
CF2	1000	356	64.4
CF3	2000	312	84.4
CF4	3000	461	84.6
CF5	4000	607	84.8

Figure 7 shows that the removal efficiency of Cs from contaminated solution is increasing with increasing the initial activity of Cs, till reach the saturation value (85%)

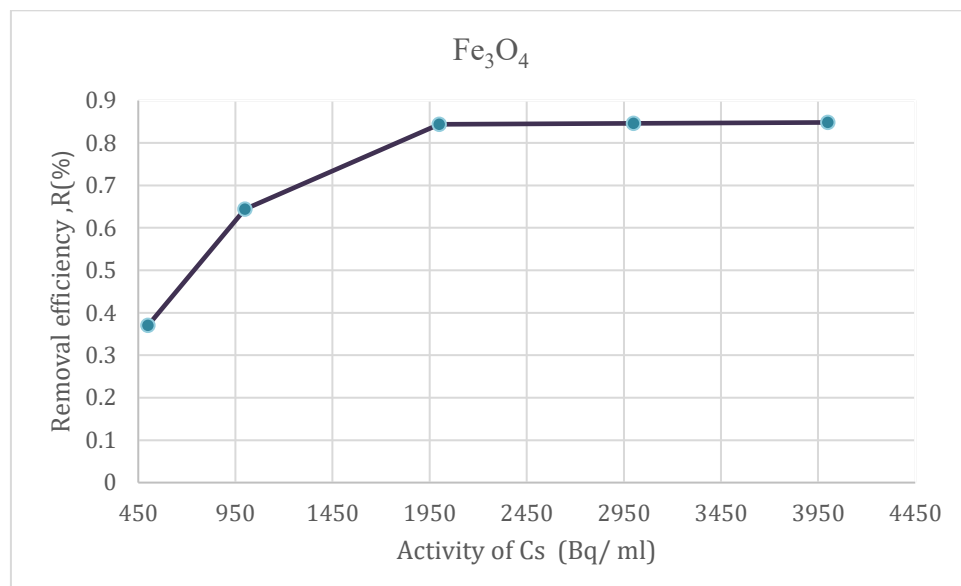


**Figure 7:** Effect of specific activity of Cs-137 on the removal efficiency of radioactive waste

###### 7- Effect of aqueous pH on the remediation process of radioactive waste

The reduction performance of Cs was also evaluated for different pH values of the contaminated water with constant absorbent mass of (0.5g), and constant contact time between nano  $\text{Fe}_3\text{O}_4$  and Cs ions of (1440 min). Table 3 shows that the removal efficiency increased as the pH of the contaminated water was increased reaching a maximum value at pH equal to 9, where the percentage reduction of Cs captured by  $\text{Fe}_3\text{O}_4$  was 82%. After that the removal efficiency decreased when the pH value increases, as shown in Table 3. This decrease was attributed to potential precipitation of cesium salts or changes in the surface charge of the adsorbent at elevated pH levels. These results showed that  $\text{Fe}_3\text{O}_4$  successfully and selectively adsorbed Cs. Then, the Cs-loaded  $\text{Fe}_3\text{O}_4$  nanoparticles magnetic were separated successfully from the contaminated water.

The results showed the efficiency of removal the cesium (Cs) using  $\text{Fe}_3\text{O}_4$  was increased with increasing pH, reaching a maximum value of 82% at a pH of 9. After this value, the efficiency of removal decreases. This action agrees with the results of other works, which also suggests that pH plays an important role in the process of adsorption. A work by Chen et al. [17] showed that the dependent of adsorption of heavy metals on iron oxide nanoparticles, on the pH value, with optimal removal observed around pH 8-9. The conclusion of their study is higher pH values reduce the contest between protons and metal ions for adsorption sites. On the contrary, Jiao et al. [18] presents that while adsorption efficiency increased with pH, it peaked at pH 8 and then decreases at higher values, similar to our results.

Additionally, a study of Li and Zhang [19] confirmed that the adsorption efficiency of many adsorbents, including  $\text{Fe}_3\text{O}_4$ , often presents a peak at a specific pH, after which further increases in pH can lead to decrease efficiency due to electrostatic repulsion or altered chemical interactions.

**Table 3:** The sample code, the pH values of contaminated water, the count rate at the peak before and after treatment ( $C_e$ ,  $C_f$ ) and the reduction percentage for Cs-137 radionuclides from water at constant mass of adsorption (nano  $\text{Fe}_3\text{O}_4$ )(0.5g) , the volume (10ml) of aqueous and contact time (1440min)

pH	$C_e(\text{Bq}/\text{ml})$	$C_f(\text{Bq}/\text{ml})$	R(%)
3	2315	1990	14.03
5	2315	1050	54.64
7	2315	553	76.11
9	2315	401	82.67
11	2315	615	73.43

#### 8- Effect of contact time on the remediation process of radioactive waste

The reduction experiment was done with different contact times between nano  $\text{Fe}_3\text{O}_4$  and Cs ions at a constant absorbent mass of (0.5g). Table 4 shows that the removal efficiency increased as the contact time increased from 30-1440 min, reaching a maximum value of 84.6% at 1440 min. This value of removal efficiency remains constant at a higher contact time of 2880 min, as shown in Table 4 and Fig.8. These results confirmed that  $\text{Fe}_3\text{O}_4$  captures Cs in the presence of mixed ion species. The magnetic separation successfully recovered the Cs-loaded adsorbent from the aqueous solvent.

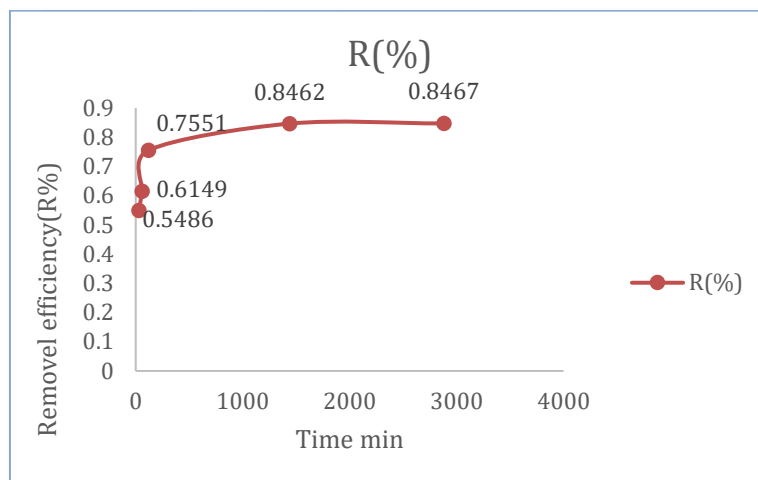
In comparing this result with those from existing literature, our findings highlight a notable trend: the removal efficiency of  $\text{Fe}_3\text{O}_4$  increased with contact time, peaking at 84.6% at 1440 minutes, after which it stabilized at 2880 minutes. This behavior is consistent with studies such as those by Wang et al. [20], which also reported improved adsorption efficiency with increased contact time but suggest that some adsorbents may continue to show enhancements beyond 1440 minutes.

Zhang et al. [21] indicated the initial increase in removal efficiency, but their results showed continued improvement removal efficiency up to 3000 minutes, suggesting that specific conditions or different adsorbents could yield varying results.

Additionally, a study by Kumar and Puri [22] demonstrated that the saturation point for other materials was reached after extended contact times, but they reported a gradual decline in efficiency after a certain period, which contrasts with this work findings of a constant efficiency at 2880 minutes.

**Table 4:** The removal efficiency values at different contact time

Contact Time (min)	$C_e$ (Bq/ml)	$C_f$ (Bq/ml)	R(%)
30	2315	1045.00	54.86
60	2315	891.45	61.49
120	2315	567.00	75.51
1440	2315	356.00	84.62
2880	2315	354.89	84.67

**Figure 8:** The removal efficiency values at different contact times.

## Conclusions

The results demonstrated that nano  $\text{Fe}_3\text{O}_4$  can effectively remove Cs-137 from radioactively contaminated water through adsorption. The optimal conditions for the remediation process were found to be: absorbent mass of 0.5g, a specific activity of 4000 Bq/ml, a pH of 9, and a contact time of 1440 min. These findings suggest that nano  $\text{Fe}_3\text{O}_4$  can be used as a promising adsorbent for the decontamination of radioactive waste, particularly in the presence of mixed ion species.

## References

- [1] Arias-Est'vez, M. E. L'opez-Periago, E. Mart'inez-Carballo, J. Simal-G'andara, J.-C. Mejuto and L. Garc'ia-R'io, Agric., Ecosyst. Environ., "The mobility and degradation of pesticides in soils and the pollution of groundwater resources," *Agriculture, Ecosystems & Environment*, vol. 123, pp.47–260, 2008
- [2] S. M. Park, J. Lee, E. K. Jeon, S. Kang, M. S. Alam, D. C. Tsang, D. S. Alessi, K. Baek, "Adsorption characteristics of cesium on the clay minerals: structural change under wetting and drying condition," *Geoderma*, vol. 340, pp. 49–54, 2019.
- [3] S. M. Abd, N. B. Naji, W. Z. Majeed, Asia H. Al-Mashhadani, "Determination of Excessive Lifetime Cancer Risk for Workers Exposed to Natural Radioactive Materials in Various Equipment in Oil and Gas Sector," *Iraqi Journal of Science*, vol. 65, no. 8, pp. 4820–4827, 2024
- [4] P. Cappelletti, G. Rapisardo, B. de Gennaro, A. Colella, A. Langella, S. F. Graziano, D.L. Bishi, M. de Gennaro, "Immobilization of Cs and Sr in aluminosilicate matrices derived from natural zeolites," *J. Nucl. Mater.*, vol. 414, pp. 451–457, 2011.
- [5] R.C. Martinez, M.T. Olgun, M.S. Rios, "Cesium sorption by clinoptilolite-richtuffs in batch and fixed-bed systems," *Desalination*, vol. 258, pp. 164-170, 2010.
- [6] S. Zhuang, Jianlong Wang, "Cesium removal from radioactive wastewater by adsorption and membrane technology," *Frontiers of Environmental Science & Engineering*, vol. 18, no. 3, pp. 38, 2024

- [7] J. Wang, Shuting Zhuang, "Removal of cesium ions from aqueous solutions using various separation technologies," *Reviews in Environmental Science and Bio-Technology*, vol. 18, no. 2, pp. 231-269, 2019.
- [8] J. Wang, S. Zhuang, Y. Liu, "Metal hexacyanoferrates-based adsorbents for cesium removal," *Coordination Chemistry Reviews*, vol. 374, pp. 430-438, 2018
- [9] M. Rashid, G. E. Sterbinsky, M. ÁG. Pinilla, Y. Cain, K. E. O'Shea, "Kinetic and Mechanistic Evaluation of Inorganic Arsenic Species Adsorption onto Humic Acid Grafted Magnetite Nanoparticles," *J. Phys. Chem. C*, vol. 122, pp. 13540–13547, 2018.
- [10] Z. Wen , J. Lu, Y. Zhang, G. Cheng, S. Huang, J. Chen, R. Xu, Y. Ming, Y. Wang, R. Chen, "Facile inverse micelle fabrication of magnetic ordered mesoporous iron cerium bimetal oxides with excellent performance for arsenic removal from water," *J. Hazard. Mater.*, vol. 383, pp. 121172, 2020.
- [11] Zaidoon H. Ibrahim, Asia H. Al-Mashhadani, "Treatment of contaminated soil with NORM of oilfields by chemical extraction method", to be published in *Baghdad Science Journal* in May, 2025.
- [12] A. Alanood Alsarayreh, K. Taisir Abbas, Saleh O. Alaswad, Sabad- Gul, A. D. Bajoga "Remove Liquid Radioactive Wastes Utilizing Nanofiltration, Ultrafiltration, and Microfiltration Membranes," *Engineering and Technology Journal*, vol. 40, no. 09, pp. 1231-1259, 2022.
- [13] N. Z. Habeeb, Asia H. Al-Mashhadani, A.M. Ali, "Natural antioxidant by scavenging free radicals activities using nano turmeric," *AIP Conference Proceedings*, vol. 2372, pp. 130018, 2021.
- [14] H. H. Alkazzaz, Asia H. Al-Mashhadani, K. H. Lateef, "Activity Treatment of Some Long-Lived Radioactive Nuclides Using Thermal Neutron Incineration," *Iraqi Journal of Science*, vol. 64, no. 6, pp. 2852–2866, 2023
- [15] Y.M. Wang, X. Cao, G.H. Liu, R.Y. Hong, Y.M. Chen, X.F. Chen, H.Z. Li, B. Xu, D.G. Wei, "Synthesis of  $\text{Fe}_3\text{O}_4$  magnetic fluid used for magnetic resonance imaging and hyperthermia," *Journal of Magnetism and Magnetic Materials*, vol. 323, pp. 2953-2959, 2011.
- [16] B. Dennis, Cullity, "Elements of X-ray Diffraction" (third ed.), Prentice-Hall International, Upper Saddle River, NJ, London, 2000.
- [17] H. Chen, et al. "pH-dependent adsorption of heavy metals on iron oxide nanoparticles," *Environmental Science and Technology*, vol. 52, no. 6, pp. 3234-3242, 2018.
- [18] Y. Jiao, et al. "Adsorption of cesium onto iron oxide: Effect of pH and ionic strength," *Journal of Hazardous Materials*, vol. 416, pp. 125896, 2021.
- [19] Q. Li, X. Zhang, "Influence of pH on the adsorption properties of various nanomaterials: A review," *Materials Science and Engineering*, vol. 112, pp. 110921. 2020.
- [20] Y. Wang, et al. "Efficient removal of heavy metals using iron oxide nanoparticles," *Journal of Hazardous Materials*, vol. 364, pp. 30-39, 2019.
- [21] L. Zhang, et al. "Adsorption behavior of heavy metals on modified iron oxide nanoparticles," *Environmental Science and Pollution Research*, vol. 27, no. 8, pp. 8900-8910, 2020.
- [22] A. Kumar, S. Puri, "Comparative study of adsorption efficiency of various nanomaterials," *Materials Today: Proceedings*, vol. 47, pp. 4567-4572, 2021.